Electronic properties and superlattice formation in the semimetal $TiSe_2$

F. J. Di Salvo
Bell Laboratories, Murray Hill, New Jersey 07974

D. E. Moncton
Bell Laboratories, Murray Hill, New Jersey 07974
and Brookhaven National Laboratory, Upton, New York 11973*

J. V. Waszczak
Bell Laboratories, Murray Hill, New Jersey 07974

(Received 18 June 1976)

Neutron-diffraction studies of $TiSe_2$ show that a second-order structural phase transition occurs at $T_0 = 202$ K involving transverse atomic displacements with wave vector $\vec{q} = (1/2,0,1/2)$. The electronic transport properties of the most nearly stoichiometric crystals show that $TiSe_2$ is a semimetal with $n_e = n_h = 10^{20}/cm^3$. Small impurity concentrations or deviations from stoichiometry reduce n_h, increase n_e, and suppress the phase transition. This reduction together with the observed displacement pattern lead us to speculate that the transition is driven by an electron-hole coupling.

I. INTRODUCTION

Recent studies of charge-density-wave (CDW) states in the layered dichalcogenides of group V*b* have given us a greater understanding of this electronically-driven lattice instability.[1-3] The equivalent group IV*b* compounds are semiconductors, except $TiSe_2$ and $TiTe_2$ which are generally accepted as semimetals,[4] and perhaps TiS_2 which remains controversial.[5] Silbernagle and Gamble[6] saw a rapid change in the ^{77}Se NMR Knight shift of $TiSe_2$ versus temperature near 200 K. Thompson[7] and Benda[8] later observed anomalies in the resistivity of $TiSe_2$. Low-temperature electron-diffraction studies show a superlattice with $a = 2a_0$ and $c = 2c_0$.[9] We have received several preprints confirming this superlattice.[10-12] Also, weak incommensurate satellite peaks have been observed at $\vec{q} \approx 0.2a^*$.[9,10]

We undertook a study of $TiSe_2$ to determine the mechanism of superlattice formation. Band-structure calculations suggest that holelike carriers will exist in the *p* band around Γ and electronlike carriers in the *d* band about the line *LM* in the Brillouin zone.[13] It is possible that the transition in $TiSe_2$ involves the carriers: a coupling of holes and electrons or electrons and electrons, forming a CDW as observed in the group V*b* compounds. We report here the physical properties (resistivity, Hall effect, thermopower, and magnetic susceptibility) of $TiSe_2$, and present neutron-diffraction data which establish the symmetry-and temperature-dependent displacements that develop below $T_0 = 202$ K. We discuss the sample preparation conditions which can lead to deviations from stoichiometry and impurity contamination. Such imperfections strongly influence the transport properties and superlattice development. A systematic study of these effects has enabled us to optimize preparation conditions, produce high-quality crystals, and derive the properties of pure $TiSe_2$. We find that $TiSe_2$ has a small band overlap and a low number of carriers—a result which helps to interpret the extreme sensitivity to impurities or deviations from stoichiometry which add a relatively large number of carriers. Further, we have correlated the varying electronic structure with the superlattice formation. When the holes are removed by the addition of electrons from impurities and excess (nonstoichiometric) Ti, the superlattice is suppressed. These results, along with the atomic displacements derived from neutron scattering measurements, suggest that the transition is driven by an electron-hole coupling.

To obtain a more complete picture of the role of the electronic structure in the superlattice formation, we have also studied the mixed system $TiSe_{2-x}S_x$. Since sulfur is more electronegative than selenium, we expect the band overlap in TiS_2 to be smaller or nonexistent. However, the resistivity of TiS_2 shows an unusual T^2 temperature dependence,[5] suggesting that it may be a semimetal. On the other hand, TiS_2 does not show any evidence for a phase transition. We find that the transition is suppressed gradually with increasing x, so that $T_0 = 0$ at $x = 0.95 \pm 0.05$. Our present results on the mixed anion system are not readily interpreted, since the unusual electronic state of TiS_2 itself is not well understood.

II. SAMPLE PREPARATION AND MEASUREMENT TECHNIQUES

The dichalcogenides of Ti have a wide range of nonstoichiometry, generally forming $Ti_{1+x}X_2$. As in TiS_2, the minimum value of x is greater than zero if the preparation temperature is too high.[5,14,15] To help ensure stoichiometry, $TiSe_2$ powder was prepared at 575 °C in excess Se.[16] Single crystals of $TiSe_2$ were grown by iodine vapor transport with excess Se (1.5 mg/cm^3 of container volume) at different growth temperatures (T_g) between 575 and 900 °C, while all $TiSe_{2-x}S_x$ crystals were grown at 600 °C. Although crystals large enough for resistivity measurements were obtained at $T_g = 575$ °C, crystals large enough for neutron scattering measurements were obtained only for $T_g \gtrsim 600$ °C.

Chemical analysis of powder $TiSe_2$ samples shows that deviations from stoichiometry which occur at high preparation temperatures are not as large as in TiS_2.[14] For example, we obtain $Ti_{1+x}Se_2$ with $x = 0.01 \pm 0.003$ at 800 °C and $x = 0.018 \pm 0.003$ at 900 °C. Below a preparation temperature of 700 °C, the deviation from 1:2 stoichiometry becomes smaller than the estimated uncertainty in measurement.

In addition to deviations from stoichiometry, some iodine is included in the crystals, presumably substituting for Se. The iodine concentration determined by neutron activation analysis is 0.3 at. % in all the samples for $600 < T_g < 900$ °C.[17] To avoid iodine contamination, some crystals were grown by direct sublimation in excess Se at 630 °C. Although these crystals are sufficient for transport measurements, they are too thin (5–10 μm) for neutron-scattering studies.

The electrical resistivity ρ and Hall coefficient R_h were measured on single crystals at cooling and heating rates of ≈ 1 K/min. Either the four-point or Van der Pauw technique[18] with ultrasonic soldered indium or silver paint contacts was used. The expected absolute accuracy of ρ(300 °K) is about 10% due to nonuniform sample thickness and contact dimensions. The magnetic susceptibility (χ) was measured by the standard Faraday method.

Elastic-neutron-scattering measurements were performed at Brookhaven National Laboratory using a conventional triple axis spectrometer with the analyzer crystal removed.

III. TRANSPORT PROPERTIES

The resistivity perpendicular to the c axis (parallel to the layers) is shown in Fig. 1 for crystals grown by iodine transport at different T_g. All the curves exhibit a peak in ρ close to 165 K. Since our chemical analysis is not accurate at small x (low T_g), we use the resistivity ratio ρ(165 K)/ρ(300 K) as a measure of sample purity and/or stoichiometry. For samples grown at $T_g = 575$ and 600 °C we find $2.75 > \rho(165)/\rho(300) > 3.0$. The data of Fig. 1 show that the peak in ρ near 165 K is rapidly reduced with increasing x.

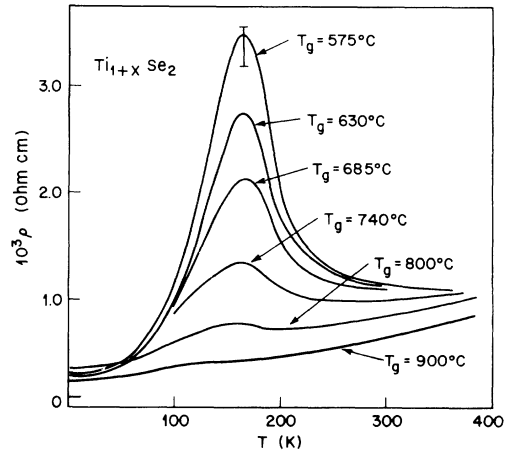

FIG. 1. Electrical resistivity perpendicular to the c axis (parallel to the layers) for crystals of $TiSe_2$ grown by iodine vapor transport at different growth temperatures (T_g). The bar on the curve for $T_g = 575$ °C represents the spread in peak values observed in crystals from the same batch.

The resistivity is smooth and peaks below T_0 indicating that the transition is not strongly first order. However $d\rho/dT$ shows a rapid change in slope at the onset of the superlattice at T_0 as determined by neutron scattering (Fig. 2). Table I lists the temperature of the minimum in $d\rho/dT$ for crystals with different T_g.

The magnetoresistance (change in resistivity in a magnetic field of 10 kG applied parallel or perpendicular to the current flow) is less than 0.1% at

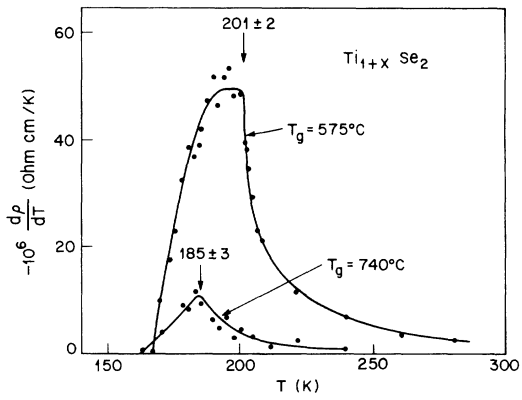

FIG. 2. Derivative of resistivity vs temperature (intervals of approximately 2 K were used in calculating $\Delta\rho/\Delta T$). The onset of the $2a_0$, $2c_0$ superlattice occurs at the rapid rise (or peak) in $d\rho/dT$.

TABLE I. Onset temperature of the superlattice T_0 decreases with increasing crystal growth temperature T_g due to increasing deviation from stoichiometry.

T_g (° C)	T_0 (break or min in $d\rho/\partial T$)
Sublimed (630 °C)	204 ± 2
575	201 ± 2
635	196 ± 3
685	192 ± 3
740	185 ± 3
800	169 ± 3
900	140 ± 5

300 K and is on the order of 0.5% at 4.2 K.

The resistivity perpendicular to the c axis of the purest $TiSe_2$ (sublimation grown) is shown in Fig. 3. By comparison with Fig. 1, it is apparent that the removal of 0.3-at.% iodine increases the resistivity at the peak, as well as the low-temperature resistivity. The inset shows $d\rho/dT$, which was calculated over 2 K temperature intervals. These data suggest that "perfect" $TiSe_2$ will show a discontinuity in $d\rho/dT$ at T_0.

All the further data presented for $TiSe_2$ were obtained with crystals grown by iodine transport at $T_g = 600$ °C, since these were used in the neutron-diffraction measurements.

The anisotropy in resistivity at 300 K is 2.5 ± 0.4, as shown in Fig. 4. This anisotropy is considerably smaller than that of group Vb or VIb layered compounds.[19,20] The slope of the resistivity parallel to the c axis ($\partial\rho_{\parallel}/\partial T$) shows a clearer break at T_0 than when the current is perpendicular to the c axis. The anisotropy calculated from

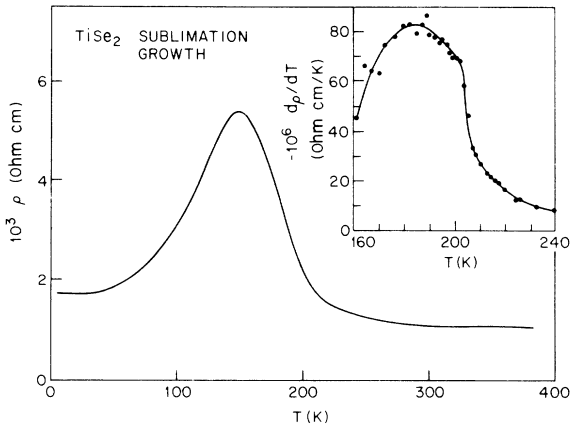

FIG. 3. Electrical resistivity perpendicular to the c axis for sublimation grown (at 630 °C) $TiSe_2$. The inset shows $d\rho/dT$ for the same sample.

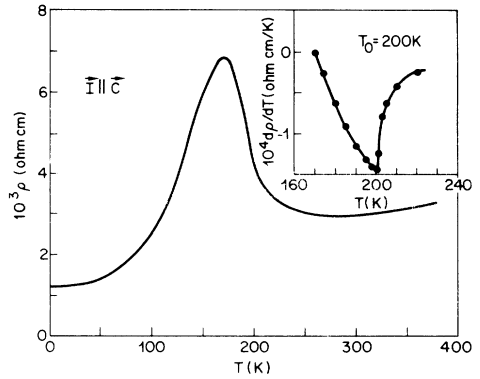

FIG. 4. Electrical resistivity parallel and perpendicular to the c axis show approximately the same temperature dependence. The anisotropy ($\rho_{\parallel}/\rho_{\perp}$) is only slightly temperature dependent and is about 2.5.

measurements of different crystals from the same batch is somewhat temperature dependent, perhaps due to small differences in the composition of the samples.

The magnetic susceptibility (χ) of $TiSe_2$ crystals with H parallel and perpendicular to the c axis, and of a $TiSe_2$ powder sample, is shown in Fig. 5. The average susceptibility calculated from $\chi_{av} = \frac{1}{3}\chi_{\parallel} + \frac{2}{3}\chi_{\perp}$ is close to that measured for the powder sample. Again, there are no discontinuities in

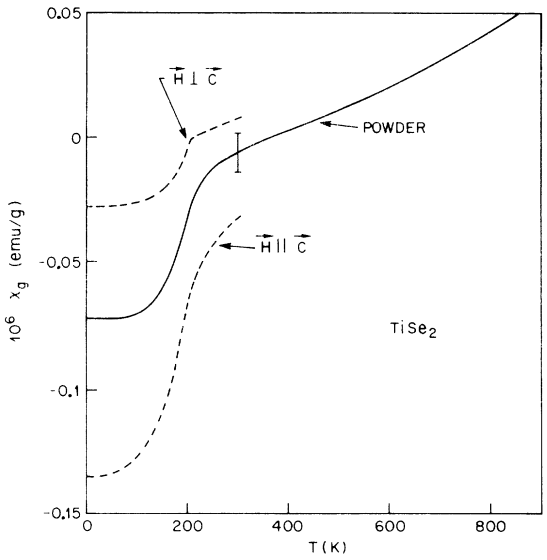

FIG. 5. Magnetic susceptibility of single crystal and powder $TiSe_2$. $d\chi/dT$ reaches a maximum at T_0. The bar on the powder data represents the absolute uncertainty of the room-temperature value of χ. While the percentage uncertainty in this value is large due to the small value of χ, the relative accuracy is close to the linewidth of the curves. A Curie-like rise in χ at low temperatures due to paramagnetic impurities has been subtracted out.

χ, but $\partial\chi/dT$ reaches a maximum at 203 ± 2 K. The decrease below T_0 is larger in $\chi_{\parallel}$ than in $\chi_{\perp}$. The difference is probably due to a large anisotropy in the carrier g values. The g values themselves may depend upon temperature, especially below T_0 where new gaps are introduced in the band structure. Without an independent measure of the g anisotropy of the electrons and holes, the change in density of states at the Fermi level can not be directly obtained from the change in χ, as previously suggested.[10]

The thermopower $S(\Delta T$ perpendicular to c axis) and the Hall coefficient R_H (I perpendicular and H parallel to the c axis) are shown in Fig. 6. The thermopower goes through a minimum with a broad plateau at low temperatures, probably due to a large negative phonon-drag contribution.[21]

The resistivity of $TiSe_{2-x}S_x$ crystals perpendicular to the c axis (Fig. 7) shows that magnitude of the peak and T_0 decrease with increasing x. The decrease of T_0 is linear for small x ($dT_0/dx = 65$ °K), but more rapid for larger x, so that the transition is completely suppressed (i.e., $T_0 \to 0$) at $x = 0.95 \pm 0.05$. For $x \geq 1.0$ the resistivity is similar to TiS_2, where the temperature dependent part of ρ is approximately proportional to $T^{2.5}$

IV. NEUTRON-DIFFRACTION MEASUREMENTS

We have measured the temperature-dependent intensity of selected superlattice peaks and the relative intensities of a large number of peaks at low temperatures.

We find a superlattice characterized by a reduced wave vector $\vec{q}_1 = (\frac{1}{2}, 0, \frac{1}{2})$ [and its symmetry equivalents: $\vec{q}_2 = (0, \frac{1}{2}, \frac{1}{2})$, and $\vec{q}_3 = (\frac{1}{2}, \frac{1}{2}, \frac{1}{2})$] developing in a continuous second-order transition at $T_0 = 201.5 \pm 0.5$ K. The temperature-dependent intensity of the strong $(\frac{3}{2}\frac{1}{2}\frac{1}{2})$ peak shown in Fig. 8

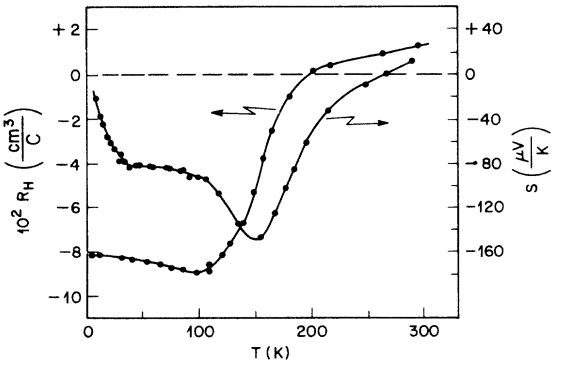

FIG. 6. Hall coefficient (R_H) and thermopower (S) of $TiSe_2$ are positive at room temperature indicating that the holes have a higher mobility than the electrons at this temperature.

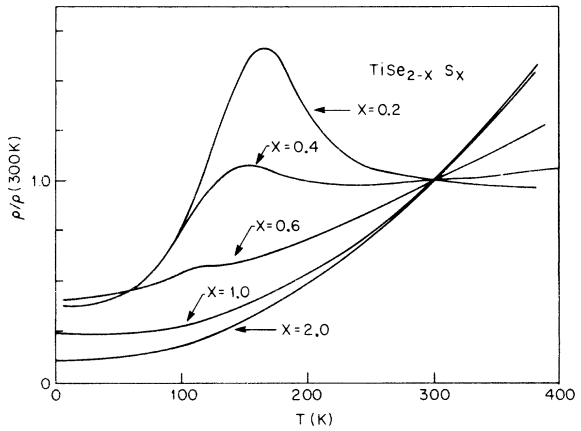

FIG. 7. Electrical resistivity of $TiSe_{2-x}S_x$ crystals perpendicular to the c axis for $0.2 \leq x \leq 2.0$. The anomaly signifying T_0 weakens rapidly and T_0 decreases to 0 at $x = 0.95 \pm 0.05$.

is proportional to the square of the order parameter for the transition. Mean-field behavior is observed in so far as $I(\frac{3}{2}\frac{1}{2}\frac{1}{2})$ is proportional to $(T_0 - T)$ over a range of at least 10 K below T_0.

The superlattice peaks have reasonably large intensities, the strongest being only a factor of 10^{-2} weaker than the strongest Bragg peak of the undistorted phase. A survey of the superlattice intensities well below T_0 indicates that no peaks occur in the $(h0l)$ plane. Since this plane contains the wave vector $\vec{q}_1 = (\frac{1}{2}, 0, \frac{1}{2})$ we conclude that the atomic displacements occurring below T_0 must be perpendicular to the $(h0l)$ plane. Symmetry constraints classify the normal modes at $\vec{q}_1$ according to four irreducible representations, two of which involve purely transverse atomic displacements. Displacement eigenvectors transforming as these two representations, denoted L_2 and L_4, are shown

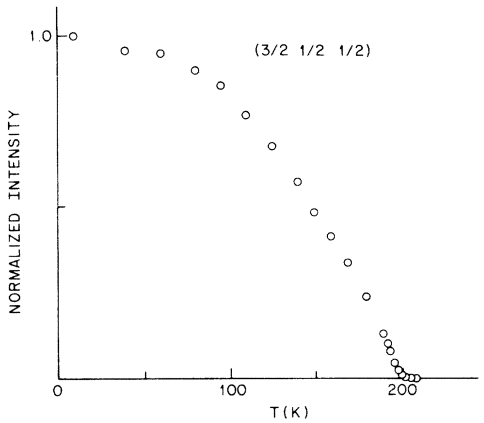

FIG. 8. Temperature dependence of the intensity of the $(\frac{3}{2}, \frac{1}{2}, \frac{1}{2})$ superlattice peak shows the second-order character of the transition.

in Fig. 9.

Assuming the atomic displacements occuring below T_0 are from a single representation, our intensity data clearly require an eigenvector of L_2 symmetry. This eigenvector contains only two independent parameters: the shift in the $\hat{y}$ direction of the Ti and Se atoms respectively. Since we observe superlattice peaks at wave vectors $\vec{q}' = (\frac{1}{2}h, \frac{1}{2}h, l)$, which can only exist by multiple processes requiring at least two wave vectors from the set $\{\vec{q}_1, \vec{q}_2, \vec{q}_3\}$, the superlattice most likely involves a microscopic superposition of displacement waves having all three wave vectors. This triple-$\vec{q}$ state can be described by expressing the atomic displacements for the kth atom in the lth unit cell as

$$\vec{u}_{lk} = \sum_{\vec{q}=\vec{q}_1,\vec{q}_2,\vec{q}_3} \vec{e}_k(\vec{q}) \cos(\vec{q}\cdot\vec{R}_l).$$

Intensity data taken at 77 K are best fit with Ti atom ($k=1$) displacement amplitude

$$\vec{e}_1(\vec{q}_1) = (0.012 \pm 0.002)a\hat{y},$$

and Se atom ($k=2,3$) amplitude

$$\vec{e}_{2,3}(\vec{q}_1) = (0.004 \pm 0.001)a\hat{y},$$

where $a = 3.535$ Å is the hexagonal lattice constant. The eigenvectors $\vec{e}_k(\vec{q}_2)$ and $\vec{e}_k(\vec{q}_3)$ have the same magnitude and are perpendicular to their respective wave vectors.

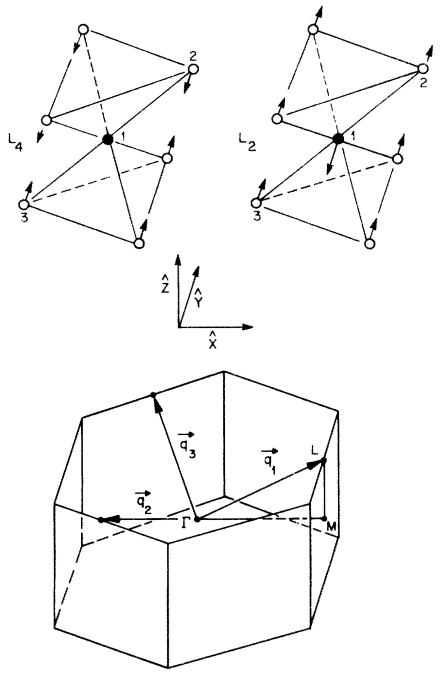

FIG. 9. Displacement eigenvectors for phonons of L_2 and L_4 symmetry are shown for a single octahedron of Ti and Se. The hexagonal Brillouin zone of $TiSe_2$ is labeled with the symmetry points and wave vectors of interest.

The displacement pattern which results from the superposition of the three distortion waves is shown in Fig. 10. We note that $\frac{3}{4}$ of the Ti and Se atoms more from their equilibrium positions in such a way as to produce three atom clusters of $TiSe_2$. The Ti-Se distance in these clusters decreases by about 0.08 Å (at 77 K) from the undistorted distance of 2.53 Å (at 300 K).

V. DISCUSSION

We first examine the normal-state properties of $TiSe_2$. In particular, the extent of band overlap and the density of electrons (or holes) are of primary importance. These parameters can be estimated from the transport data presented here if we make some assumptions concerning the mobility and band structure.

In a two-band model of a semimetal with n_h and n_e the density of holes and electrons, respectively, ρ, R_H, and S may be written rather generally as[21,22]

$$\sigma = (1/\rho) = |e|(n_h \mu_h + n_e \mu_e), \tag{1}$$

$$R_H = \frac{1}{|e|c}\left(\frac{n_h\mu_h^2 - n_e\mu_e^2}{(n_h\mu_h + n_e\mu_e)^2}\right), \tag{2}$$

$$S = \frac{S_h n_h \mu_h - |S_e| n_e \mu_e}{n_h \mu_h + n_e \mu_e}, \tag{3}$$

where μ_h and μ_e are the mobilities of the holes and electrons and S_h and S_e are the individual thermopowers of the holes and electrons (all perpendicular to c axis).

For stoichiometric defect-free $TiSe_2$, we have $n_e = n_h$. We assume that the material prepared at low T_g reasonably satisfies this condition. There

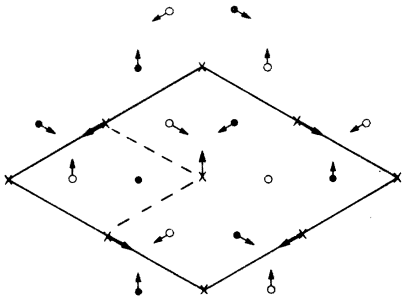

x = Ti; o = Se (up); • = Se (down)

FIG. 10. Schematic representation of the low-temperature displacements of Ti and Se in a single layer viewed from above. The upper Se sheet is denoted by ○, the lower Se sheet by •, and the middle Ti sheet by ×. The pattern is derived from the sum of three plane-wave distortions of L_2 symmetry. The displacements at 77 K are 0.085 Å for Ti and 0.028 Å for Se parallel to the plane of the layer.

are too many parameters in Eqs. (1), (2), and (3) to determine each from the data. Rather we estimate n_e at a particular temperature where $R_H = 0$, by assuming a value of μ_e. When $R_H = 0$ near 204 K, Eq. (2) gives $\mu_e = \mu_h$ and then Eq. (1) becomes $\sigma = 2|e|n_e\mu_e$. Choosing a value of μ_e typical of other layered compounds at 200 K (TiS_2 $\mu_e \sim 15 cm^2/V$ sec,[23] $MoSe_2$ p-type $\mu_h \sim 15$ cm^2/V sec),[24] we estimate $n_e = 10^{20}$, or 6×10^{-3} electrons per Ti. This value indicates that only a small overlap of the valence and conduction bands occurs. Above T_0 = 202 K, R_H is temperature dependent and positive indicating that the electron mobility decreases more rapidly with temperature than the hole mobility. At 200 K, $S_h < |S_e|$, and if we assume that S_h and S_e are temperature independent [as is approximately the case in semimetallic Bi (Ref. 25)], we again conclude that μ_e decreases more rapidly than μ_h, so that S becomes positive near 270 K.

A rough estimate of the Fermi energy of the carriers (E_F^e and E_F^h) can be made using the calculated density of states of $1T - TaS_2$ and $TiSe_2$ near the bottom of the d band and the top of the p band. The density of states is obtained from the fine-grid density of states calculated for $1T - TaS_2$ by Mattheiss,[13] but scaled by the difference in overall density of states obtained for $TiSe_2$ by Myron and Freeman[26] where larger energy intervals were reported. Using $n_e = 10^{20}/cm^3$, we find $E_F^e \approx 300$ K and $E_F^h \approx 600$ K. These estimates should be correct within a factor of 2. At this low density of carriers and small overlap, it seems likely that both n and E_F are temperature dependent due to both thermal expansion and the difference in the density of states in the p and d band (again the temperature dependence is similar to that found in other semimetals such as bismuth).[25,27,28] Both the large temperature dependence of χ and the continued decrease in ρ well above 200 K further support this possibility. It is possible, however, that some of these changes, especially in ρ close to 200 K, are due to pretransition fluctuation effects. The resistivity increases below T_0 presumably due to the appearance of gaps over portions of the Fermi surface, which reduces the number of carriers. With decreasing temperature, ρ continues to increase until the thermal generation of carriers across the increasing gaps becomes small. Then at lower temperatures a metallic-like resistivity is observed from those portions of the Fermi surface that are not disrupted by gaps. The fact that the magnetoresistance is small at low temperatures shows that, within a two-band model,[22] the electron and hole mobilities remain relatively small, less than approximately 400 cm^2/V sec at 4.2 K.

Deviations from stoichiometry would increase the number of electrons and decrease the number of holes. Assuming each excess Ti to donate four electrons to the bands, we estimate that the density of holes becomes zero at $x = 0.03$. From the stoichiometry data and the resistivity curves of Fig. 1, we estimate that T_0 has decreased to zero at $x = 0.035 \pm 0.005$. This implies that the presence of the holes is fundamental to the formation of the superlattice.

The atomic displacements also suggest that the transition is driven by an electron-hole coupling. Such a coupling would occur with the observed q vector, since electron pockets are expected to exist at L and holes at Γ. An electron-hole coupling would be expected to lead to a decrease in the Ti-Se bond length. Such a decrease would increase the basic bonding-antibonding gap, uncrossing the primarily Se-based p and Ti-based d bands, resulting in a decrease in the density of both electrons and holes.

This transition is most likely another variety of CDW instability, where the electron-phonon interaction is strong enough to produce a distortion when the electron and hole Fermi surfaces are near nesting. Unlike other CDW transitions where incommensurate wave vectors are found, the present superlattice appears at a zone-boundary point. Transitions driven by coupled electron-phonon instabilities in which the bare electronic susceptibility peaks in the vicinity of the zone boundary may result in superlattices which have, at inception, exactly the zone-boundary wave vector. This fact results from the umklapp energy gained by locking to the commensurate structure.[29] In the zone-boundary case, this lock-in energy is proportional to the square of the order parameter and is not a higher-order effect, as in the group Vb compounds (i.e., $TaSe_2$) where the wave vector is some other fraction of a recriprocal lattice vector.[1-3,31] Within, this model, $TiSe_2$ can continue to exhibit the same zone-boundary superlattice when the Fermi surfaces are altered by nonstoichiometry or impurities. Consequently, we would not observe a change in the wave vector of the distortion when the electronic structure is altered by doping, as is the case for the Vb compounds.[32]

Electron electron coupling from M to L (in the next electron pocket) has also been proposed as the mechanism for this instability.[10,11] While we can not definitively choose a particular model at the present time, we feel that the data strongly suggest that the electron-hole coupling is important, as originally suggested by Wilson.[9] We note that the transition has some similarities to that observed in VS near 900 K,[33,34] where the transition is also thought to be driven by an electron hole coupling.[30] The $TiSe_2$ transition may also be

characterized as an excitonic electron-hole interaction resulting in a semimetal to semimetal transition,[35] but this is equivalent to a CDW when the bands overlap, as they do in the present case.

We have not yet determined the source of the weak incommensurate peaks observed in electron diffraction at $q \approx 0.2a^*$. These peaks appear below T_0, but apparently disappear below 100 K.[9,10] There are no obvious changes in the transport properties or the order parameter of the superlattice below T_0 to associate with the existence of these peaks.

This study also prompts questions concerning the nature of the conductivity in TiS_2. The small band overlap suggested here for $TiSe_2$ would lead one to expect no overlap in TiS_2 because of the larger electronegativity difference of the cation and anion. The resistivity of $TiSe_{2-x}S_x$ shows no extra anomalies, which might be expected near the composition where the bands first uncross. For example some "excitonic insulator" phase might occur[9,35] which would result in a semiconductor to semiconductor phase transition. However, this excitonic phase may be suppressed by nonstoichiometry or the anion disorder. In these particular crystals, it is certain that some iodine is included, since the inclusion occurs in both end members. It is also possible that the problems of nonstoichiometry are more severe in such mixed systems. While the possibility of an excitonic insulator in this system is based on the expectation that TiS_2 should be a small band-gap semiconductor, we note that TiS_2 has quite unusual transport properties that suggest semimetallic conduction.[5] Perhaps the properties of TiS_2 itself are related in some way to an excitonic electron-hole instability of the small band gap, or to some as yet unproven defects that may occur in both TiS_2 and $TiSe_2$. Further work in this mixed anion system is continuing with the hope of increasing our understanding of both TiS_2 and $TiSe_2$.

VI. CONCLUSIONS

The properties of $TiSe_2$ are quite sensitive to small deviations from stoichiometry or impurities such as iodine. Crystals grown at low temperatures (≈ 600 °C) show a pronounced peak in resistivity below T_0, in the purest samples $R(\text{peak}) = 4.85\,R(300\text{ K})$. While the density of holes and electrons in probably temperature dependent, we find that n_e and n_h in the purest $TiSe_2$ samples are on the order of $10^{20}/\text{cm}^3$ with $E_F^e \simeq \frac{1}{2}E_F^h = 300$ K.

The elastic neutron scattering results show that transverse atomic displacements develop at wave vector $\vec{q} = (\frac{1}{2}, 0, \frac{1}{2})$ in a second-order transition at $T_0 = 202$ K. The decrease of T_0 with increasing electron density and the displacement pattern suggest that the transition is driven by an electron-hole coupling.

Inelastic-neutron-scattering measurements are underway to study the lattice dynamics associated with the transition and the effects of varying electronic structure. Other detailed studies such as optical reflectance and transmission, and ^{77}Se NMR will be published shortly.

ACKNOWLEDGMENTS

Throughout this work we have benefited from discussions with J. A. Wilson and acknowledge his stimulation of our work on this problem. The efforts of G. W. Hull, Jr. in measuring the thermopower of $TiSe_2$ are appreciated. We also thank J. D. Axe, T. M. Rice, and A. H. Thompson for several useful conversations.

---

*Work at Brookhaven National Laboratory performed under the auspices of the U. S. Energy Research and Development Administration.

[1]J. A. Wilson, F. J. Di Salvo, and S. Mahajan, Adv. Phys. 24, 117 (1975).
[2]D. E. Moncton, J. D. Axe, and F. J. Di Salvo, Phys. Rev. Lett. 34, 734 (1975).
[3]P. M. Williams, G. S. Parry, and C. B. Scruby, Philos. Mag. 29, 695 (1974).
[4]D. L. Greenaway and R. Nitsche, J. Phys. Chem. Solids 26, 1445 (1965).
[5]A. H. Thompson, Phys. Rev. Lett. 35, 1786 (1975).
[6]B. G. Silbernagel and F. R. Gamble (unpublished).
[7]A. H. Thompson (unpublished).
[8]J. A. Benda, Phys. Rev. B 10, 1409 (1974).
[9]J. A. Wilson and S. Mahajan (unpublished); and F. J. Di Salvo, D. E. Moncton, J. A. Wilson, and J. V. Waszczak, Bull. Am. Phys. Soc. 21, 261 (1976).
[10]K. C. Woo, F. C. Brown, W. L. McMillan, R. J. Miller, M. J. Schaffman, and M. P. Sears (unpublished).
[11]W. Y. Liang, G. Lucovsky, R. M. White, W. Stutius, and K. R. Pisharody, Philos. Mag. 33, 493 (1976).
[12]P. M. Williams, *Physics and Chemistry of Layered Crystal Structures*, Vol. 2 (Reidel, New York, 1976).
[13]L. F. Mattheiss, Phys. Rev. B 8, 3719 (1973). (We assume the band structure will not drastically change if the p-d band gap is reduced through zero.)
[14]Y. Jeannin, Ann. Chim. 7, 57 (1962).
[15]A. H. Thompson, F. R. Gamble, and C. R. Symon, Mater. Res. Bull. 10, 915 (1975).
[16]F. K. McTaggart and A. D. Wadsley, Aust. J. Chem. 11, 445 (1958). At 575 °C, $TiSe_3$ does not appear to be stable, in contrast to TiS_3.
[17]This result is similar to that found for TiS_2, where from 0.1 to 0.5-at.% iodine is included, depending upon the preparation conditions. (A. H. Thompson, private

communication).
[18]L. J. Van der Pauw, Phillips Tech. Rev. 20, 220 (1958).
[19]J. Edwards and R. F. Frindt, J. Phys. Chem. Solids 32, 2217 (1971).
[20]B. L. Evans and P. A. Young, Proc. R. Soc. A 284, 402 (1965).
[21]R. D. Barnard, *Thermoelectricity in Metals and Alloys* (Wiley, New York, 1972).
[22]J. M. Ziman, *Electrons and Phonons* (Oxford U. P., Oxford, 1963).
[23]L. E. Conroy and K. C. Park, Inorg. Chem. 7, 459 (1968).
[24]W. T. Hicks, J. Electrochem. Soc. 111, 1058 (1964).
[25]C. F. Gallo, B. S. Chandrasekhar, and P. H. Sulter, J. Appl. Phys. 34, 144 (1963).
[26]H. W. Myron and A. J. Freeman, Phys. Rev. B 9, 481 (1974).
[27]B. Abeles and S. Meiboom, Phys. Rev. 101, 544 (1956).
[28]M. S. Dresselhaus, *The Physics of Semimetals and Narrow Gap Semiconductors*, edited by D. L. Carter and R. T. Bate (Pergamon, New York, 1971).
[29]The lock-in or commensurability energy was first considered for the case of a spin-density wave by C. Herring, in *Magnetism*, Vol. 4, edited by G. T. Rado and H. Suhl (Academic, New York, 1966), p. 340; later by S. H. Liu for the case of a CDW (see Ref. 30).
[30]S. H. Liu, Phys. Rev. B 10, 3619 (1974).
[31]W. L. McMillan, Phys. Rev. B 12, 1187 (1975).
[32]F. J. Di Salvo, J. A. Wilson, B. G. Bagley, and J. V. Waszczak, Phys. Rev. B 12, 2220 (1975).
[33]H. F. Franzen, C. Haas, and F. Jellinek, Phys. Rev. B 10, 1248 (1974).
[34]H. F. Franzen, J. Solid State Chem. 13, 114 (1975).
[35]B. I. Halperin and T. M. Rice, Solid State Phys. 21, 115 (1968); Rev. Mod. Phys. 40, 755 (1968).